An Approach to Understanding Bond Length/Bond Angle Relationships

William A. Shirley,[†,‡] Roald Hoffmann,*[,‡] and Vladimir S. Mastryukov[§]

Computational Science and Engineering Group, Cornell Theory Center, and Department of Chemistry and Material Science Center, Cornell University, Ithaca, New York 14853-1301, and Department of Chemistry and Biochemistry, The University of Texas, Austin, Texas 78712-1167

Received: October 14, 1994[⊗]

In many studies the relationship between a bond's length and the angle formed with an adjacent bond has been shown to be inverse; larger bond angles result in shorter bond lengths. Mastryukov and co-workers, however, have found some bonds that lengthen at extreme angles. In this work, the bond length/bond angle relationship was reexamined to gain understanding of the normal behavior and this occasional turnover in behavior at large angles. The correlation between bond lengths and adjacent bond angles in CX_4, CXH_3, and CHX_3 (X = H, Cl, F) has been studied by extended Hückel and *ab initio* Hartree−Fock/STO-3G techniques. In these molecules, the angle between three of the bonds and the fourth unique bond was varied, thus retaining C_{3v} symmetry. We examined the overlap populations between each of the atoms and the central carbon as a function of angle. In the case of the *ab initio* calculations, we also allowed all bond lengths to relax. We present arguments to explain the normal and direct behavior on the basis of overlap populations, Walsh diagrams, *ab initio* optimized bond lengths, and consideration of the nonbonded, X···X, interactions. We are able to explain the anomalous behavior at large angles in two ways: (a) from a decomposition of the molecular orbitals and the delicate balance of s and p character in them and (b) from the adjustments the electronic structure makes to the uncomfortably short X···X contacts.

The nature of the relationship between bond length R_1 (or R_2) and the angle to an adjacent atom (θ) or atoms, defined in **1**, is an old problem. Interest in this area has renewed as experimentalists begin to make highly strained molecules.[1−8]

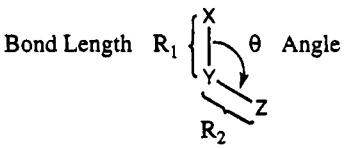

1

The normal bond length/bond angle relationship is an *inverse* one, *i.e.*, shorter X−Y (or Y−Z) bond lengths are associated with larger X−Y−Z angles. One of the most dramatic manifestations of this occurs in the bicyclobutane system.[6,9−13] Irngartinger *et al.* demonstrated that the length of the hinge bond of bicyclobutane derivatives such as **2** is inversely proportional to an external angle ϕ.[12]

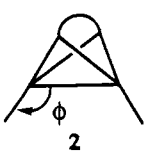

2

Indeed, the shortest bond length between saturated carbons is 1.408 Å and is found in a bicyclobutane derivative, **3**, that has very large external angles.[6,12,14]

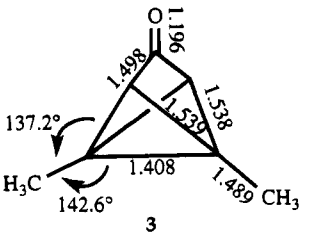

3

The extreme shortness of this hinge bond is due in part to interaction of the cyclopropane (bicyclobutane) orbitals with the acceptor carbonyl group.[15] However, large C−C−C angles may be associated with short C−C bonds, even in the absence of such conjugation. For instance, despite substantial steric strain, the central C−C bond in the coupled bicyclobutane (**4**) is 1.440 Å.[2,16,17]

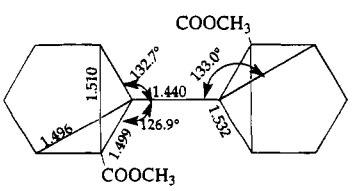

4

An inverse bond length/bond angle relationship has also been obtained in most theoretical studies,[14,18−20] especially the important ones of Wiberg and co-workers[9,21,22] and Schleyer and co-workers.[14,23] Mastryukov, Boggs, and co-workers have used *ab initio* HF-SCF calculations to systematically study the

[†] Cornell Theory Center, Cornell University.
[‡] Department of Chemistry and Material Science Center, Cornell University.
[§] Permanent address: Laboratory of Electron Diffraction, Department of Chemistry, Moscow State University, Moscow 119899, Russia.
[⊗] Abstract published in *Advance ACS Abstracts,* February 15, 1995.

0022-3654/95/2099-4025$09.00/0

relationship between bond angles and bond lengths for a variety of aliphatic molecules,[24] including A_4H_8 (A = C, Si, Ge), AH_2X_2 (A = C, Si; X = F, Cl), AX_3 (A = N, P), and AX_2 (A = O, S; X = H, CH_3, F, Cl).[25-31] They found that, for these molecules, the bond length/bond angle relationship initially is characterized by normal inverse behavior (see **5**). Curiously, some molecules experience a turnover at large angles, beyond which bond *elongation* occurs with further increases in bond angle, the so-called direct behavior. We have also observed a weak minimum in the rather different but related case of a metal−metal quadruple bond.[32]

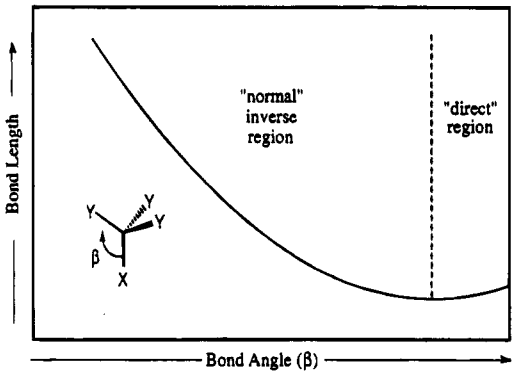

5

To understand both the normal (inverse) effect and its reversal at large bond angles, we chose to perform a computational study of several carbon-centered systems, a series of substituted methanes, using both the extended Hückel and Hartree−Fock methods. The Hartree−Fock/SCF method implemented at the STO-3G level[33-35] (no electron correlation) in general gives reasonably accurate geometries with little computational expense. Mastryukov has demonstrated that the quality of the basis set used with the Hartree−Fock method is not a significant factor in the appearance of the turnover region in his model.[27] We tested our model with the LCAO STO-3G basis and a larger split valence with polarization, 6-31G**, basis set. We found larger basis sets yield shorter lengths for most bonds, but do not substantially change the qualitative picture. Baird found similar results in his examination of the potential energy surface of several AX_2 molecules.[36] Consequently, for computational efficiency we chose the STO-3G basis.

There are some signs, however, of significant changes in C−C bond lengths in strained molecules with the degree of correlation included.[16,17,37] Schleyer reproduced the bond elongation that we found,[38] using a density functional technique implemented in *Gaussian 92/DFT*.[33,39-42] We examined the effect of correlation at the Møller−Plesset second-order level. The MP2/6-31G** optimized bond lengths are longer than those from HF/STO-3G and shorter than those of HF/6-31G**. The bond length/bond angle curves are qualitatively the same as those from the HF/6-31G** model. Duchovic, Hase, and Schlegel examined the potential energy surface of the dissociation of methane with the 6-31G** basis set and several different orders of perturbation theory.[43] They found that, through the fourth order, "electron correlation plays, at best, only a minor role in determining the optimized geometry" as the hydrogen is removed. A much more elaborate calculation by Brown and Truhlar using a multireference method found a small effect when an H had been pulled away 2.5 Å from the carbon in methane.[44] Since the C−H bond distances in our model are always considerably shorter than that, we concluded that rigorous inclusion of correlation energy is not significant.

The extended Hückel method[45-51] is parametrized to experimental data and, thus, presumably includes some electron correlation, but not in a very well-defined way. This semiempirical method has been used successfully in the construction of Walsh diagrams to explain trends in geometry with angular variation.[52] The results from extended Hückel and *ab initio* methods, as we will see, are consistent. We thus believe that we possess a qualitatively accurate picture of the phenomenon.

Geometrical Preliminaries

In the studies of Mastryukov and Boggs, the angle α affecting the bond length in question was defined between two of the atoms, as in **6**, and the molecules possessed C_{2v} symmetry. There

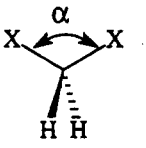

6

is an inherent ambiguity in this formulation because as α changes, the angles between X and the H's also change. The bicyclobutane derivative (**3**) shows this complexity with two external angles and three different bond lengths.

We chose instead to probe the bond length/bond angle relationship by studying an umbrella distortion, where an angle β is defined between the handle (X) and the outstretched struts (Y):

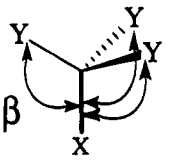

7

We also imposed C_{3v} symmetry, so that the three Y atoms are equivalent. We had used the same model to study $SiAl_4^{8+}$ in a paper on the $CaAl_2Si_2$-type compounds[53] and a similar C_{4v} distortion in our more recent paper on the pyramidality of multiply bonded dinuclear metal complexes of the type M_2X_8, M_2X_8L, and $M_2X_8L_2$.[32] Similar models (with fixed bond lengths) were used by Mårtensson to study methane[54] and by Schleyer and Bremer in their important study of ethane deformation.[14] Our umbrella model has only three structural parameters, one angle (β) and two bond lengths (the handle, C−X, and the strut, C−Y).

Note that there is nothing unique about the deformation coordinate studied. Wiberg's discussion on bending in methane suggests other models.[22] In addition to the unsymmetric bend that had been used originally by Mastryukov and the umbrella mode that we are now using, other modes could have been used, such as the symmetric or antisymmetric bends. However, our model contains a smaller number of parameters and is, thus, easier to interpret.

We decided to look at both optimized bond distances (HF calculations only) and Mulliken overlap populations (HF and EH both); the EH-optimized distances are not reliable. We varied the β angles from 50° to ~155° and allowed the other geometric parameters to relax. The constraint on the upper limit is set by failure to achieve convergence of the Hartree−Fock

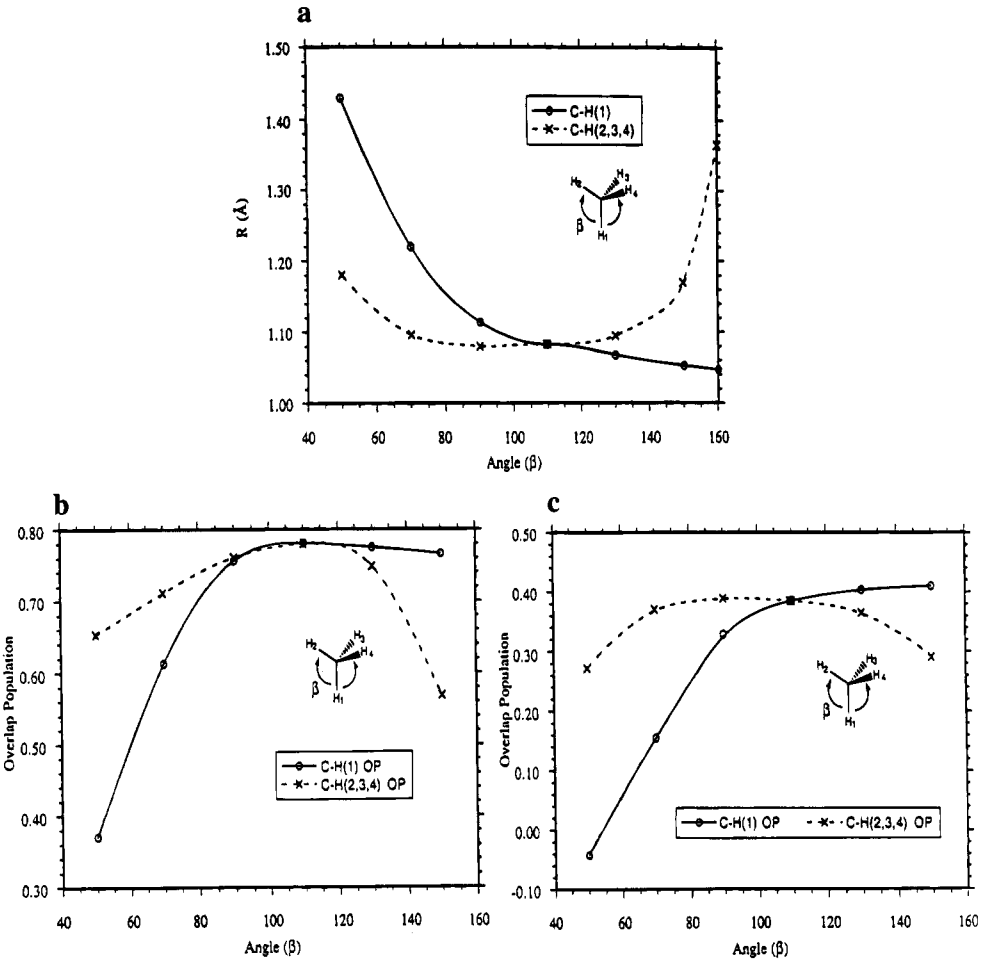

Figure 1. Optimized bond lengths and overlap populations for methane as a function of the umbrella angle, β: (a) Hartree–Fock/STO-3G-optimized bond lengths; (b) extended Hückel overlap populations (with bond lengths fixed); (c) Hartree–Fock OPs with bond lengths optimized for each angle.

method at larger angles. Direct behavior or a turnover region, when present, was observed for β values beyond ~145°. This is the same range of extreme angles where Mastryukov and Boggs observed the phenomenon.

The hydrocarbon systems that we examined were methane (**8**) and substituted methanes **9**–**11**, where X = F, Cl.

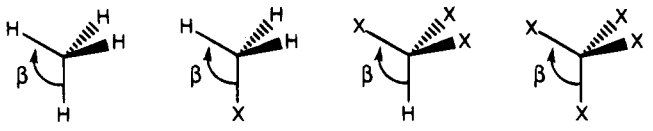

8 **9** **10** **11**

Computational Results and Discussion

In the optimized distances of methane as a function of β, we see only the normal inverse bond length/bond angle behavior for the handle bond. This may be seen in Figure 1a, where the solid line refers to the unique handle bond and the dashed line represents the strut bonds. The overlap population (OP) curves (Figures 1b,c), from both the *ab initio* and extended Hückel calculations for the C–H handle bond, rise; a larger overlap population, of course, implies a shorter bond. The EH curve has a slight turnover in the OP that is not present in the HF results.

Fragment MO Analysis and Hybridization. To understand the normal inverse behavior, let us look first at a partitioning of CH_4 into CH_3 and H, as shown in **12**.

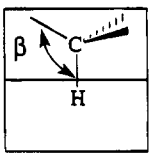

12

The orbitals of CH_3 are very well-known.[55] The HOMO singly occupied in the methyl radical is the $2a_1$. Shown in **13** for β = 110°, it has the expected appearance, being a hybrid of C 2s and $2p_z$ (95% $2p_z$). Its overlap with the H 1s of the handle is superb (0.488 at β = 110°), and it is primarily this interaction—$2a_1$ on CH_3 with 1s on H—that forms the new handle C–H bond.

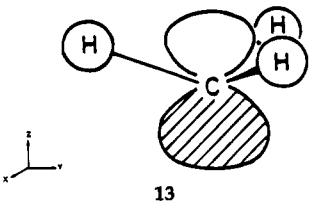

13

Figure 2 shows the $1s(H)-2a_1(CH_3)$ fragment molecular orbital (FMO) overlap as a function of β. Note the following: (a) The overlap is large at all angles. This is unexpected at small β, since then the H 1s overlaps with the back side of the $2a_1$. But small orbital pictures are misleading. The $2a_1$ is

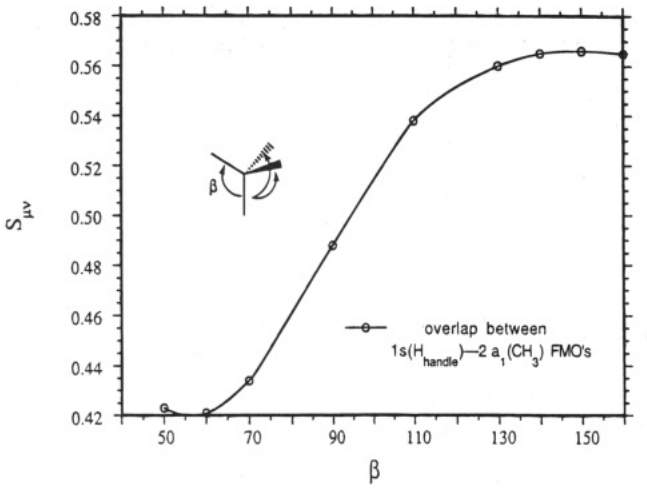

Figure 2. Overlap between the fragment molecular orbitals 1s(H) and $2a_1(CH_3)$ of CH_4 as a function of the angle β, calculated by the extended Hückel method.

mostly $2p_z$ at all β (the 2s character of CH_3 FMO $2a_1$ rises monotonically from 0 at $\beta = 90°$ to 7% at $\beta = 50°$ (or 130°)). The $2p_z$ contribution to the $1s-2a_1$, overlap is dominant, and this is high even when the CH_3 lobe points "the wrong way". (b) Note the monotonic increase in $1s-2a_1$ overlap with β over a wide range of angles. This is the explanation of the normal effect: as β increases, the $1s-2a_1$ overlap rises, and a stronger (therefore shorter) C−H bond forms. (c) There appears to be an asymptote to the overlap at large β, but no clear turnover in it. We do not have a simple explanation of why the overlap levels off.

What about the classical, valence bond-based (VB) hybridization argument? We think it would run in its most simplistic version as follows:[54,56−58] The handle C−H bond is to be thought of as being formed by a CH_3 hybrid lobe and a hydrogen. The % s character in that lobe is zero at $\beta = 90°$ (a trigonal planar CH_3 radical) and should rise monotonically with β. The more s character in the CH_3 lobe, the better its overlap with the handle H. Thus, the simplest VB model also predicts the normal inverse bond length/bond angle relationship.

A reviewer has correctly called us to task for this oversimplification of valence bond theory. The actual hybridization in bonds or radical lobes is different for each molecule and depends on the atoms; in general, bonds prefer more s character, radical lobes prefer p.[59] In a more complete VB treatment, one still predicts the normal inverse behavior.

In the bicyclobutane derivative **3**, we can think of the hinge bond (1.408 Å) and two other endocyclic bonds (1.538 and 1.539 Å) as struts and the exocyclic bond (1.489 Å) as a handle bond. Thus, two of the strut bonds are of normal length, ~1.538 Å, and one is of record-setting length, 1.408 Å. It has been previously shown that the bicyclobutane hinge bond has mostly p character.[20,60−66] This implies that the handle bond has the increased s character that our arguments suggest.

A Second MO Analysis Based on a Walsh Diagram for Methane. Consider a Walsh diagram for the umbrella deformation of methane (Figure 3). The orbitals of methane are well-known.[67] At lowest energy there is $1a_1$, a bonding C2s−H combination. This orbital is followed by $1t_2$, $C2p_{x,y,z}-H$ bonding; the corresponding antibonding combinations are now shown in the figure. As the symmetry is reduced to C_{3v} (for β less or greater than 109.5°), $1t_2$ splits into e + a_1. The $2a_1$ orbital contributes to the $C-H_{handle}$ bonding along with $1a_1$. The $C-H_{strut}$ bonding derives principally from the 1e orbital. So it is easy to understand that the strongest $C-H_{strut}$ bonding is at

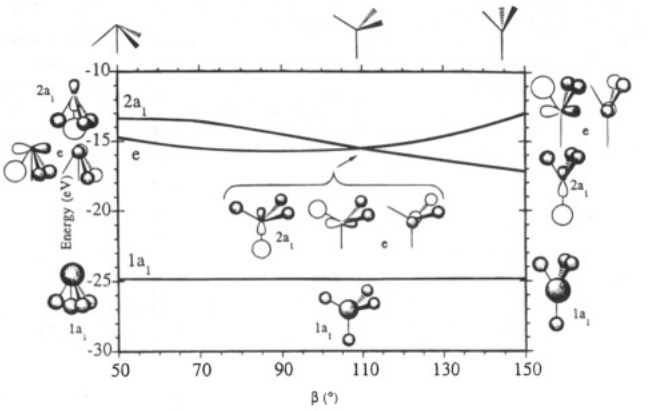

Figure 3. Walsh diagram for the umbrella distortion of methane. Pictured are the thumbnail sketches of the molecular orbitals for β less than, equal to, and greater than 109.5°.

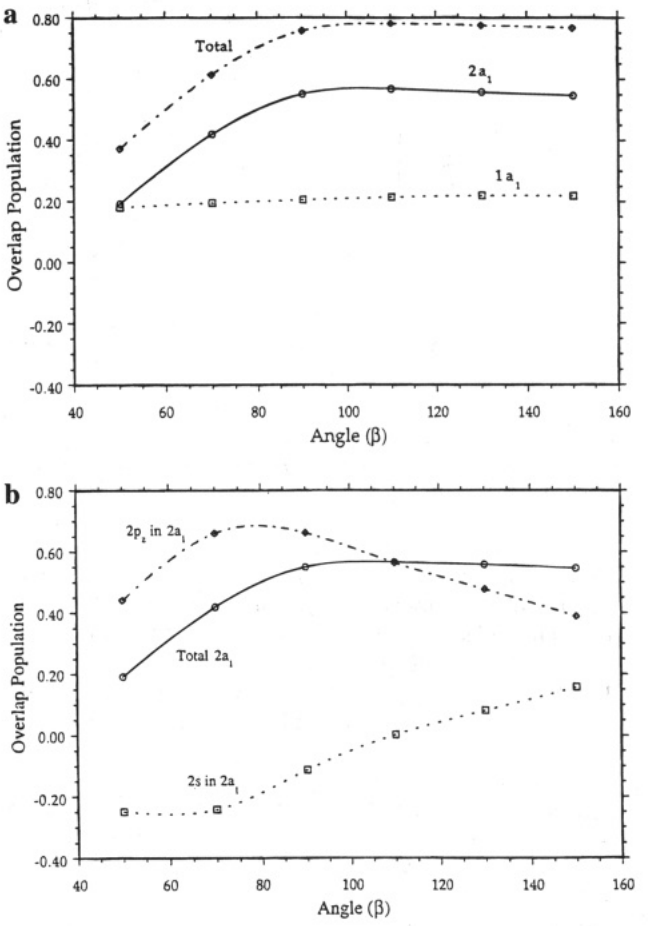

Figure 4. Decomposition $C-H_{handle}$ overlap population of methane as a function of β: (a) contributions to the $C-H_{handle}$ OP from the molecular orbitals $2a_1$ and $1a_1$; (b) atomic orbital contributions to the $2a_1$ decomposition of the $C-H_{handle}$ OP.

$\beta \sim 90°$ (see Figure 1), since this is the point of optimum $C2p_{x,y}-H$ overlap. This is not a new argument, but it is similar to one that has been presented before by Schleyer and Bremer.[14]

The $C-H_{handle}$ bond is a little more complicated to analyze. Figure 4 (top) shows a decomposition of this overlap population by molecular orbital ($1a_1$ and $2a_1$). We note that the $1a_1$ MO contributes a constant amount to the $C-H_{handle}$ OP, so that the trend observed is determined entirely by $2a_1$. The bottom of Figure 4 shows the breakdown of the $2a_1$ $C-H_{handle}$ by the type of orbital, 2s or $2p_z$, on C. The shape of the $2a_1$ orbital as a

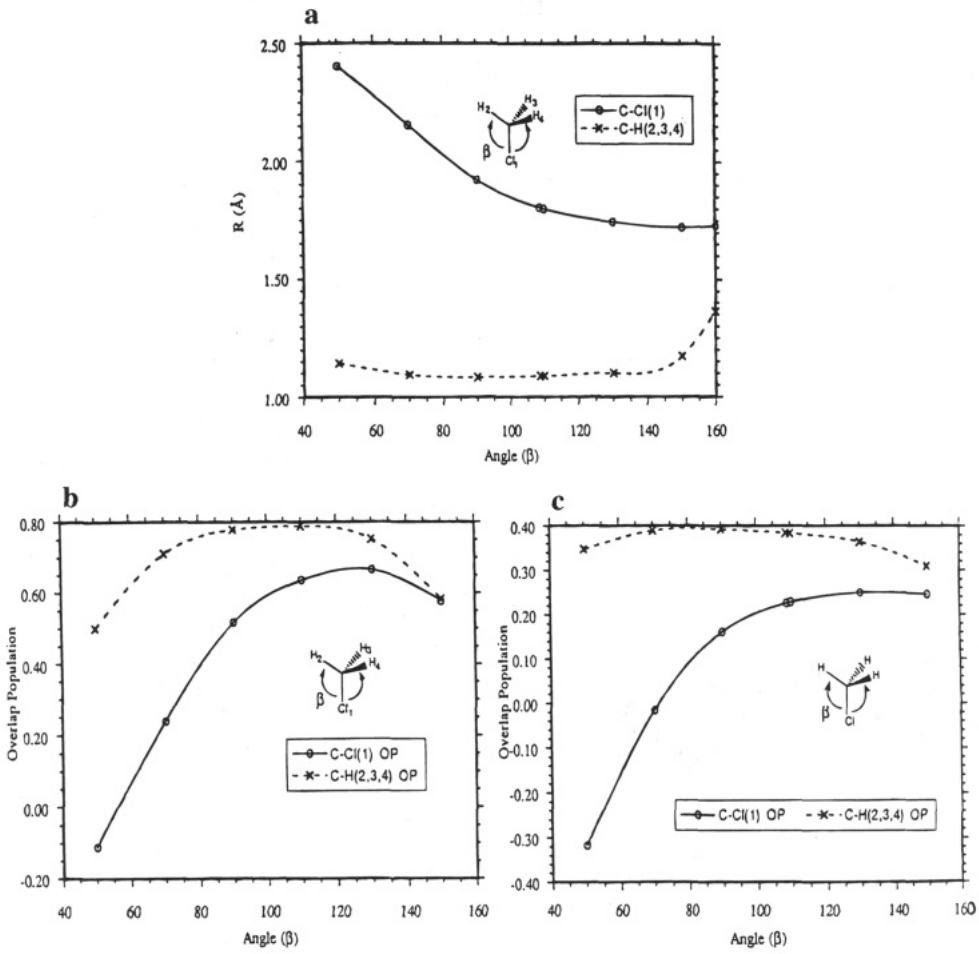

Figure 5. Optimized distances and overlap population for chloromethane as a function of β: (a) Hartree−Fock/STO-3G-optimized bond lengths; (b) extended Hückel overlap populations (with bond lengths fixed); (c) Hartree−Fock/STO-3G OPs with bond lengths optimized at each angle.

function of β is sketched in **14** and accounts for the behavior one sees.

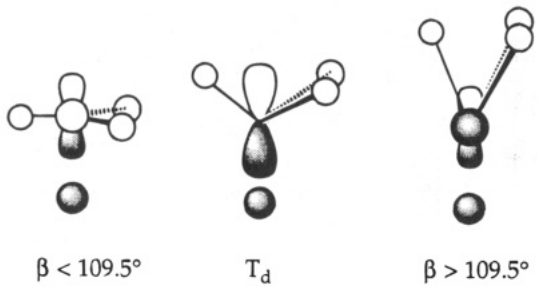

14

At the tetrahedral geometry, there is no 2s character in $2a_1$. For $\beta < 109.5°$, the 2s mixing is out-of-phase with H_{handle}, yielding a negative contribution to the C−H_{handle} OP. For $\beta > 109.5°$, the 2s mixing is in-phase. Thus, the 2s contribution to the OP rises monotonically with β. The $2p_z$ contribution is maximal near $\beta = 90°$. The net result of 2s and $2p_z$ contributions is a composite OP curve that peaks near the tetrahedral geometry and then is pretty flat at larger β. Whether the OP actually rises (*i.e.*, the C−H_{handle} bond is stronger and, presumably, shorter) in the region $\beta > 109.5°$ is a delicate balance of the 2s (rising) and $2p_z$ (falling) contributions to the OP. This is why we observe a range of behavior in the bond lengths—sometimes only the normal inverse effect, sometimes a slight turnover.

Chloromethane and More Elaborate Calculations. We next examined $CClH_3$ with the Cl in the handle (Figure 5). Note the very slight turnover beyond $\beta = 150°$: very slight indeed in the HF-optimized distances and OPs and more pronounced in the EH OPs. CCl_4 shows only normal inverse behavior (Figure 6).

In general, in these compounds the elongation is small in magnitude. For the handle the elongation is ~0.01 Å for F and Cl and ~0.04 Å for hydrogen. The absolute accuracy of the HF/STO-3G model is estimated to be *ca.* ±0.03 Å and *ca.* ±1.3° for *equilibrium* geometries, but this may not be an appropriate measure of the correctness of our conclusions.[68,69] We are looking at the change in bond length rather than the absolute length, and for the former we believe the model is reasonably reliable. It is possible that the abnormal geometries (very small or very large β) lead to artifacts.[37] However, consistent results between the two methods suggest that the small region of direct behavior is a real phenomenon.

In order to look for artifacts, we ran a few more elaborate calculations on methane and the chloro-substituted molecules. Our calculations with the larger split valence with polarization basis set 6-31G** yield shorter lengths for most bonds, but do not substantially change the qualitative picture. With this larger basis set, CH_4 displays a small (0.0085 Å) elongation of the handle bond at 150°. The effect of correlation was examined at the Møller−Plesset second-order level. The MP2/6-31G** bond lengths are intermediate between the Hartree−Fock STO-3G and 6-31G** values. The bond length/bond angle curves are qualitatively the same as those from the HF/6-31G** model. Prompted by our study, Schleyer[38] examined methyl chloride with the Becke3LYP/6-31G** implementation[33,39−42] of density functional theory and confirmed our observations. He found

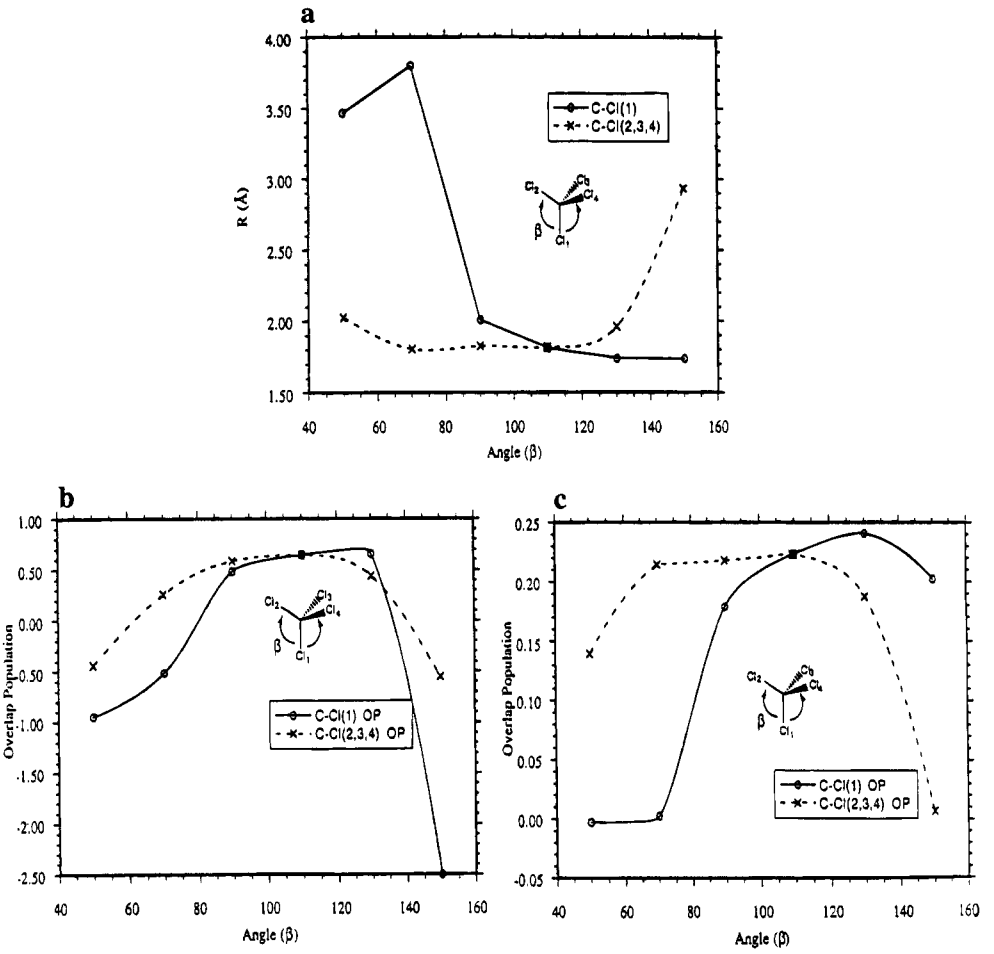

Figure 6. Optimized distances and overlap populations for carbon tetrachloride as a function of the angle β: (a) Hartree–Fock/STO-3G-optimized bond lengths; (b) extended Hückel overlap populations (with bond lengths fixed at the experimental values); (c) Hartree–Fock/STO-3G OPs with bond lengths optimized at each angle.

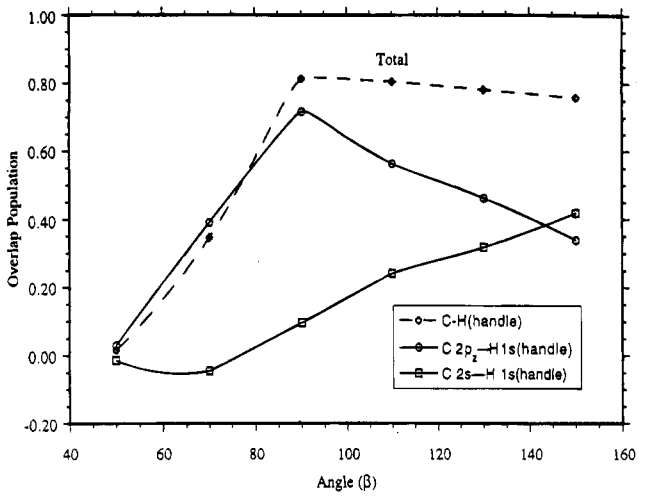

Figure 7. Decomposition of the C–H extended Hückel overlap population into atomic orbital contributions as a function of the umbrella angle, β.

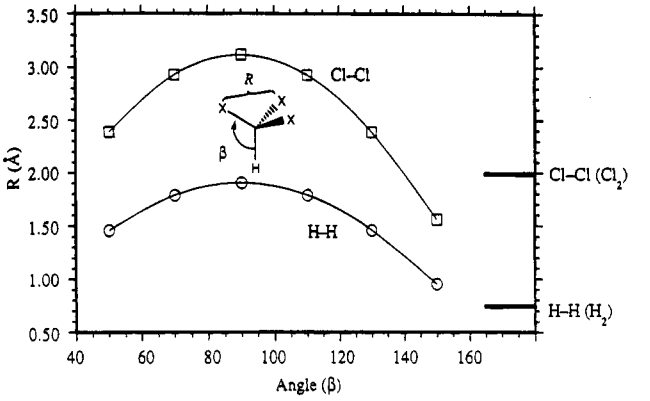

Figure 8. Intrastrut distances for methane and chloroform as a function of the angle β, with C–H and C–Cl distances fixed at 1.1 and 1.8 Å, respectively. For comparison, bond lengths for diatomic chlorine and diatomic hydrogen are shown at right.

that the equilibrium C–Cl distance of 1.80 Å decreases to 1.68 Å at 150° and then lengthens to 1.69 Å at 160°.

In our HF/STO-3G and extended Hückel calculations, CH_4 exhibits only a small deviation from the standard inverse bond length/bond angle relationship. In contrast, Figure 7 shows the distinct region of direct behavior that is exhibited by $CHCl_3$. The p contribution falls off more steeply for the system that exhibits direct behavior. Comparison with the previously shown decomposition into s and p contributions for methane indicates that the balance of s and p contributions is a sensitive one.

Steric Problems as a Possible Cause of the Turnover. There is still another way to think about the turnover in the bond length/bond angle relationship. The turnover region may be due to our imposing unreasonably small intramolecular distances between the struts.[36] In Figure 8, we show the interstrut distance (H···H or Cl···Cl) in CH_4 and $CHCl_3$, assuming "normal" C–H and C–Cl distances of 1.1 and 1.8 Å, respectively. The bond lengths of H_2 and Cl_2 are also marked on the graph. It is clear that at large β these atoms are forced

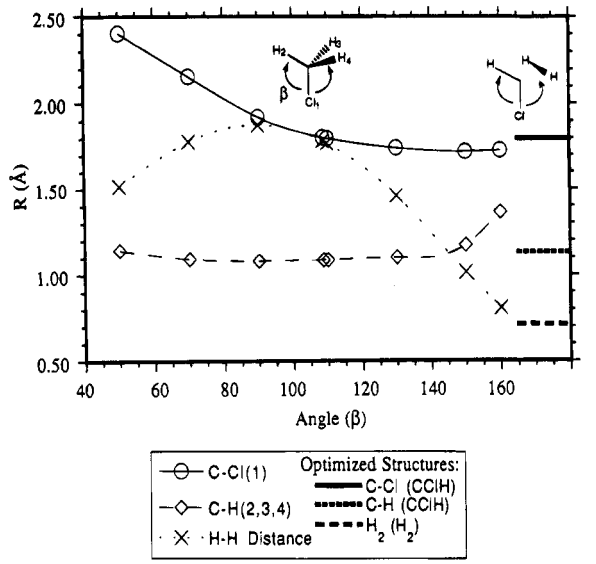

Figure 9. Hartree–Fock/STO-3G-optimized bond distances for chloromethane as a function of the angle β. For comparison, bond lengths from the optimized structures of the excited state singlet of (chloromethyl)carbene and diatomic hydrogen are shown at right.

too close to each other. In fact, we think that for very large β a better description of the bonding in these highly distorted molecules may be one of interacting CHCl + Cl_2 (or CClH + H_2 or CYX + X_2) (**15**) or CH + H_3 (or CY + X_3)[70] (**16**) fragments.

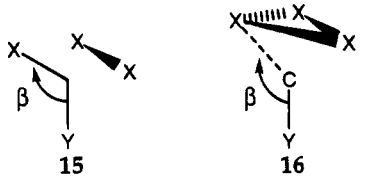

Now at first sight this change in bonding would *not* be expected to lead to a turnover from an inverse to a direct regime. Taken at face value, **15** implies a change to sp^2 hybridization at the central carbon (a reviewer correctly points out that this is true only for the singlet state of the carbene, and only if the C–X bonds and the carbene lone pair have identical preferences for p character), which would lead one to expect a shorter C–Y bond, not the lengthening that calculations give for very large β. However, as we will see, detailed consideration of the problem leads to the conclusion that the X–X bonding may weaken the C–Y bond.

We probe the notion of intrastrut interactions first for $CClH_3$. For $CClH_3$, the fragments within the symmetry constraint are CHCl and H_2:

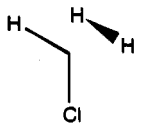

We compared the bond lengths of our optimized structures of $CClH_3$ to the optimized bond lengths found in the isolated fragments CClH and H_2. As β increases above 150°, as shown on the graph (Figure 9), the H–H interstrut distance is compressed to that of the STO-3G-optimized H_2. Note that as β increases, the C–Cl distance decreases so that it actually becomes a little *below* the C–Cl equilibrium distance in CClH. At large β, that distance begins to increase again. Above 150°, within the constraints of the C_{3v} symmetry imposed, the

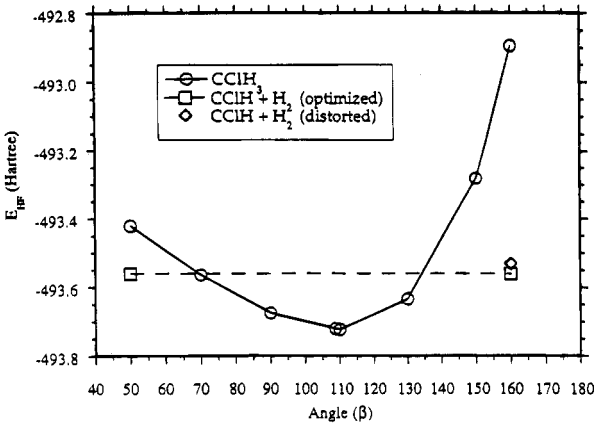

Figure 10. Hartree–Fock/STO-3G energy (○) of chloromethane as a function of the angle β, with bond lengths optimized. Sum of HF/STO-3G energies of the singlet excited state of (chloromethyl)carbene and of diatomic hydrogen with the optimized structures (□). Sum of HF/STO-3G energies of the singlet excited state of (chloromethyl)-carbene and of diatomic hydrogen (◇) with the C–Cl, C–H, and H–H distances and the Cl–C–H angle from the distorted $CClH_3$ structure (160°).

molecule is trying to break into the two fragments. The bond lengths of these fragments, as with many radicals, are slightly longer than those of the parent molecules.[71,72]

In studies by Schleyer communicated to us, the multiconfiguration CASSCF method confirmed the desire of $CClH_3$ to break up with $\beta = 160°$. Optimization of the structure at this angle resulted in a loss of C_{3v} symmetry. While at smaller angles it was found that only one configuration was significant in the description of the wavefunction, at this large angle, after the symmetry was broken, an additional configuration became significant.[38]

From the *ab initio* total energies we can see the driving force for the fragmentation of $CClH_3$ at large angles. Above 140°, the total energy of $CClH_3$ has risen above the sum of the optimized ground state energies of CClH and H_2. Even if we distort the two fragments, CClH and H_2, to have the same C–H, C–Cl, and H–H bond lengths and the same Cl–C–H angle as those found in the $CClH_3$ molecule, the energy of the distorted molecule is still higher than the sum of the energies of the fragments (Figure 10). Were the C_{3v} symmetry not imposed and H_2 allowed to move away, the optimization would have yielded two separate non-interacting species. Although our model is clearly limited to C_{3v} systems, we believe that our explanation for this specific region of direct behavior is applicable to a wider variety of systems, including those studied by Mastryukov, Boggs, and co-workers.

Mastryukov has suggested[28] that experimental results[73] provide evidence that, in general, fluorinated molecules would be more likely than chlorinated molecules to have a region of direct bond length/bond angle behavior.[77] Our calculations (not reported in detail) indicate that CF_4 behaves normally, like CCl_4 and CH_4, while CFH_3 and CHF_3 exhibit the direct behavior, as found in $CClH_3$ and $CHCl_3$.

We sought support from experimental work for our interpretation that the inverse/direct behavior is related to a balance of s and p character in the C handle bond as a function of the angle β. Indeed, spectroscopic evidence does give some support to this notion. The magnitude of the elongation can be roughly correlated to the ^{13}C–H coupling constants from NMR spectroscopy (see the relationship reviewed in the classic paper on hybridization by Bent).[59] The coupling constants for C–H bonds of substituted methane have been used to estimate the s character, α_H^2, at equilibrium geometries.[63–66] The valence

TABLE 1: Extended Hückel Parameters Used in the Calculations

atom	orbital	H_{ii} (eV)	ζ_{i1}	ref
H	1s	−13.60	1.300	48
C	2s	−21.40	1.625	48
	2p	−11.40	1.625	
Cl	3s	−26.30	2.183	75
	3p	−14.20	1.733	
F	2s	−40.00	2.425	76
	2p	−18.10	2.425	

bond framework behind the theory of coupling constants is fairly primitive, but it is interesting nevertheless to trace the consequences of this kind of reasoning. Assuming additivity of the s character ($3\alpha_H^2 + \alpha_X^2 = 1$ or $3\alpha_X^2 + \alpha_H^2 = 1$), we can estimate the s character of the C−X bonds at equilibrium. This distribution of s character in the handle and strut bonds is related to an intrinsic preference of the ligands at equilibrium.[74] It appears that this preference is partially retained as the molecules are deformed. In molecules where the struts and the handle atoms are the same ($\alpha_{handle}^2 = \alpha_{strut}^2$), little or no elongation occurs. In molecules where the handle and strut atoms are not the same, the difference between the s character of the handle and strut bonds ($\alpha_{handle}^2 - \alpha_{strut}^2$) at equilibrium appears to be related to the magnitude of the elongation observed.

A question remains: Why is the turnover region either very small or not observed in CH_4, CCl_4, or CF_4? We do not have a satisfactory answer for this question. The manifestation of direct of inverse behavior must be connected to the relative energies of the fragments or the steepness of the potential energy surfaces near the stressed geometry. However, an examination of the force constants of the handles and a comparison of the energies of the various species at 150° did not reveal a systematic difference between the molecules that do and do not show direct behavior.

Finally, although the angles where the direct effect was observed are extreme, we should not that bicyclobutane derivative **3** has an exterior angle of ~141°. This is only 4° or 5° smaller than the beginning of the range where we observed the behavior. We thus present a challenge to experimentalists to make still more highly strained molecules that will allow observation of the exotic behavior that we have calculated.

Acknowledgment. This research was supported by the National Science Foundation, the Cornell Theory Center, and the Cornell Materials Science Center under Grant ASC-921102. R.H. and W.A.S. thank the Cornell Theory Center for time on their IBM RISC System/6000 serial cluster and their Kendall Square Research KSR1 parallel computer. We especially thank IBM for their generous donation of an IBM RISC System/6000 Model 37t with GT4x graphics and Warren Hehre of Wave-Function, Inc., for providing us with his Spartan computational chemistry code. W.A.S. thanks Mary Reppy for extensive scientific and editorial contributions. V.S.M. is grateful to the Robert A. Welch Foundation and to Professor J. E. Boggs for his hospitality and support during his two visits 1991−1992 and 1993−1994 at the University of Texas.

Appendix

Extended Hückel calculations were performed with the CACAO molecular orbital program,[50,51] with parameters taken from the Alvarez list[49] and collected in Table 1. Bond lengths for the extended Hückel calculations were as follows: C−H, 1.1 Å; C−Cl, 1.8 Å; C−F, 1.4 Å.

References and Notes

(1) Ermer, O.; Lex, J. *Angew. Chem., Int. Ed. Engl.* **1987**, *26*, 447−449.
(2) Ermer, O.; Bell, P.; Schäfer, J.; Szeimies, G. *Angew. Chem., Int. Ed. Engl.* **1989**, *28*, 473−476.
(3) Gilardi, R. *J. Am. Chem. Soc.* **1988**, *110*, 7232−7234.
(4) Kaszynski, P.; Michl, J. *J. Am. Chem. Soc.* **1988**, *110*, 5225−5226.
(5) Irngartinger, H.; Goldmann, A.; Schappert, R.; Garner, P.; Dowd, P. *J. Chem. Soc., Chem. Commun.* **1981**, *1981*, 455−456.
(6) Irngartinger, H.; Lukas, K. L. *Angew. Chem., Int. Ed. Engl.* **1979**, *18*, 694−695.
(7) Blount, J. F.; Mislow, K. *Tetrahedron Lett.* **1975**, *11*, 909−912.
(8) Blount, J. F.; Maryanoff, C. A.; Mislow, K. *Tetrahedron Lett.* **1975**, *11*, 912−916.
(9) Cox, K. W.; Harmony, M. D.; Nelson, G.; Wiberg, K. B. *J. Chem. Phys.* **1969**, *50*, 1976−1980.
(10) Suenram, R. D.; Harmony, M. D. *J. Am. Chem. Soc.* **1973**, *95*, 4506−4511.
(11) Kabuto, C.; Tatsuoka, T.; Murata, I.; Kitahara, Y. *Angew. Chem., Int. Ed. Engl.* **1974**, *13*, 669−670.
(12) Irngartinger, H.; Reiner, J.; Rodewald, H.; Paik, Y. H.; Dowd, P. *J. Am. Chem. Soc.* **1987**, *109*, 6547−6548.
(13) Dowd, P.; Irngartinger, H. *Chem. Rev.* **1989**, *89*, 985−996.
(14) Schleyer, P. v. R.; Bremer, M. *Angew. Chem., Int. Ed. Engl.* **1989**, *28*, 1226−1228.
(15) Stohrer, W.-D.; Hoffmann, R. *J. Am. Chem. Soc.* **1972**, *94*, 1661.
(16) Xie, Y.; Schaefer, H. F., III *Chem. Phys. Lett.* **1990**, *168*, 249−252.
(17) Xie, Y.; Schaefer, H. F., III *Chem. Phys. Lett.* **1989**, *161*, 516−518.
(18) Alden, R. A.; Kraut, J.; Traylor, T. G. *J. Am. Chem. Soc.* **1968**, *90*, 74−82.
(19) Rüchardt, C.; Beckhaus, H.-D. *Angew. Chem., Int. Ed. Engl.* **1985**, *24*, 529−616.
(20) Rathna, A.; Chandrasekhar, J. *J. Mol. Struct. (THEOCHEM)* **1991**, *228*, 249−258.
(21) Wiberg, K. B.; Ellison, G. B. *Tetrahedron* **1974**, *30*, 1573−1578.
(22) Wiberg, K. B.; Ellison, G. B.; Wendoloski, J. J. *J. Am. Chem. Soc.* **1976**, *98*, 1212−1218.
(23) Budzelaar, P. H. M.; Cremer, D.; Wallasch, M.; Würthwein, E.-U.; Schleyer, P. v. R. *J. Am. Chem. Soc.* **1987**, *109*, 6290−6299.
(24) Alcolea Palafox, M.; Boggs, J. E.; Mastryukov, V. S. *14th Austin Symp. Mol. Struct.* **1992**, 76.
(25) Mastryukov, V. S. *J. Mol. Struct.* **1991**, *263*, 343−347.
(26) Mastryukov, V. S.; Samdal, S. *J. Mol. Struct.* **1992**, *268*, 395−399.
(27) Mastryukov, V. S.; Boggs, J. E. *J. Mol. Struct.* **1993**, *300*, 141.
(28) Mastryukov, V. S.; Alcolea Palafox, M.; Boggs, J. E. *J. Mol. Struct. (THEOCHEM)* **1994**, *304*, 261.
(29) Shchapin, I. Y.; Mastryukov, V. S. *J. Mol. Struct.* **1992**, *268*, 307−310.
(30) Shchapin, I. Y.; Mastryukov, V. S. *Vestn. Mosk. Univ., Ser. 2: Khim.* **1992**, *33*, 235−241.
(31) Mastryukov, V. S.; Shchapin, I. Y. *Vestn. Mosk. Univ., Ser. 2: Khim.* **1991**, *32*, 569−572.
(32) Mota, F.; Novoa, J. J.; Losada, J.; Alvarez, S.; Hoffmann, R.; Silvestre, J. *J. Am. Chem. Soc.* **1993**, *115*, 6216−6229.
(33) Frisch, M. J.; Trucks, G. W.; Head-Gordon, M.; Gill, P. M. W.; Wong, M. W.; Foresman, J. B.; Johnson, B. G.; Schlegel, H. B.; Robb, M. A.; Replogle, E. S.; Gomperts, R.; Andres, J. L.; Raghavachari, K.; Binkley, J. S.; Gonzalez, C.; Martin, R. L.; Fox, D. J.; Defrees, D. J.; Baker, J.; Stewart, J. J. P.; Pople, J. A. *Gaussian 92*, Revision D.2; Gaussian, Inc.: Pittsburgh, PA, 1992.
(34) Hehre, W. J.; Stewart, R. F.; Pople, J. A. *J. Chem. Phys.* **1969**, *51*, 2657−2664.
(35) Hehre, W. J.; Burke, L. D.; Shusterman, A. J. A. *Spartan Tutorial, Version 3.0*; Wavefunction, Inc.: Irvine, CA, 1993.
(36) Baird, N. C. *Inorg. Chem.* **1989**, *28*, 1224−1227.
(37) Xie, Y.; Schaefer, H. F., III; Aped, P.; Chen, K.; Allinger, N. L. *Int. J. Quant. Chem.* **1992**, *42*, 953−963.
(38) Schleyer, P. v. R. Universität Erlangen-Nürnberg, personal communication, 1994.
(39) Vosko, S. H.; Wilk, L.; Nusair, M. *Can. J. Phys.* **1980**, *58*, 1200.
(40) Lee, C.; Yang, W.; Parr, R. G. *Phys. Rev. B* **1988**, *37*, 785.
(41) Becke, A. D. *J. Chem. Phys.* **1993**, *98*, 5648.
(42) Becke, A. D. *Phys. Rev. A* **1988**, *58*, 3098.
(43) Duchovic, R. J.; Hase, W. L.; Schlegel, B.; Frisch, M. J.; Raghavachari, K. *Chem. Phys. Lett.* **1982**, *89*, 120−125.
(44) Brown, F. B.; Truhlar, D. G. *Chem. Phys. Lett.* **1985**, *113*, 441−446.
(45) Ammeter, J. H.; Bürgi, H.-B.; Thibeault, J. C.; Hoffmann, R. *J. Am. Chem. Soc.* **1978**, *100*, 3686−3692.
(46) Hoffmann, R.; Lipscomb, W. N. *J. Chem. Phys.* **1962**, *36*, 3489.
(47) Hoffmann, R.; Lipscomb, W. N. *J. Chem. Phys.* **1962**, *36*, 2179.
(48) Hoffmann, R. *J. Chem. Phys.* **1963**, *39*, 1397.
(49) Alvarez, S. *Tables of Parameters for Extended Hückel Calculations*; Universitat de Barcelona: Barcelona, Spain, 1993.
(50) Mealli, C.; Proserpio, D. M. *J. Chem. Educ.* **1990**, *67*, 3399.

(51) Mealli, C.; Proserpio, D. M. *CACAO (Computer Aided Composition of Atomic Orbitals)*, Firenze, Italy, 1990.
(52) Mehrotra, P. K.; Hoffmann, R. *Theor. Chim. Acta* **1978**, *48*, 301−321.
(53) Zheng, C.; Hoffmann, R.; Nesper, R.; Schnering, H.-G. v. *J. Am. Chem. Soc.* **1986**, *108*, 1876−1884.
(54) Mårtensson, O. *Acta Chem. Scand.* **1970**, *24*, 3116−3122.
(55) Jorgensen, W. L.; Salem, L. *The Organic Chemist's Book of Orbitals*; Academic Press: New York, 1973.
(56) Mårtensson, O.; Öhrn, Y. *Theor. Chim. Acta* **1967**, *9*, 133−139.
(57) Mårtensson, O.; Brändas, E. *Chem. Phys. Lett.* **1969**, *3*, 315−318.
(58) Coulson, C. A.; White, R. *Mol. Phys.* **1970**, *18*, 577.
(59) Bent, H. A. *Chem. Rev.* **1961**, *61*, 275−311.
(60) Paddon-Row, M. N.; Houk, K. N.; Dowd, P. *Tetrahedron Lett.* **1981**, *22*, 4799−4802.
(61) Newton, M. D.; Schulman, J. M. *J. Am. Chem. Soc.* **1972**, *94*, 773−778.
(62) Newton, M. D.; Schulman, J. M. *J. Am. Chem. Soc.* **1972**, *94*, 767−773.
(63) Juan, C.; Gutowsky, H. S. *J. Chem. Phys.* **1962**, *37*, 2198−2208.
(64) Muller, N.; Pritchard, D. E. *J. Chem. Phys.* **1959**, *31*, 768−771.
(65) Closs, G. L.; Closs, L. E. *J. Am. Chem. Soc.* **1963**, *85*, 2022−2023.
(66) Closs, G. L.; Larrabee, R. B. *Tetrahedron Lett.* **1965**, *4*, 287−296.
(67) Gimarc, B. M. *J. Am. Chem. Soc.* **1971**, *93*, 593−599.
(68) Hehre, W. J.; Radom, L.; Pople, J. A. *Ab Initio Molecular Orbital Theory*; Wiley: New York, 1986.
(69) Schaefer, H. F., III *Crit. Eval. Chem. Phys. Struct. Inf.* **1974**, 591−602.
(70) At this moment we are not concerned with the charge on the fragments, which might not be neutral (*e.g.*, H_3^+).
(71) Bartell, L. S.; Kuchitsu, K. *J. Chem. Phys.* **1962**, *37*, 691−696.
(72) Bartell, L. S. *J. Chem. Educ.* **1968**, *45*, 754−767.
(73) Davis, M. J.; Rankin, D. W. H.; Cradock, S. *J. Mol. Struct.* **1990**, *238*, 273−287.
(74) Root, D. M.; Landis, C. R.; Cleveland, T. *J. Am. Chem. Soc.* **1993**, *115*, 4201−4209.
(75) Summerville, R. H.; Hoffmann, R. *J. Am. Chem. Soc.* **1976**, *98*, 7240.
(76) Anderson, A. B.; Hoffmann, R. *J. Chem. Phys.* **1974**, *60*, 6271.
(77) The results cited actually provide no evidence regarding direct behavior because the range of angles in these structures, determined by electron diffraction, is between 92° and 104°. These angles are much smaller than those necessary to induce the direct behavior, if we trust the calculations. No real bond elongation has been observed.

JP942776Q